Isolation and Structure of Rhizobactin 1021, a Siderophore from the Alfalfa Symbiont *Rhizobium meliloti* 1021

Magnus Persmark,[†] Paul Pittman,[‡] Jeffrey S. Buyer,[§] Bernhard Schwyn,[⊥] Paul R. Gill, Jr.,[∥] and J. B. Neilands*

Contribution from the Division of Biochemistry and Molecular Biology, 401 Barker Hall, University of California, Berkeley, California 94720

Received October 27, 1992

Abstract: Rhizobactin 1021, a novel siderophore from the nitrogen-fixing alfalfa symbiont *Rhizobium meliloti* 1021, was isolated and structurally characterized by a combination of chemical and spectroscopic techniques. The compound is a citrate derivative in which the distal carboxyl groups of the molecule are amide linked to two different side chains. One of these is 1-amino-3-(*N*-hydroxy-*N*-acetylamino)propane, and the other is 1-amino-3-(*N*-hydroxy-*N*-(*E*)-2-decenylamino)propane. The structure of rhizobactin 1021 was determined as (*E*)-4-[[3-(acetylhydroxyamino)propyl]-amino]-2-hydroxy-2-[2-[3-[hydroxy(1-oxo-2-decenyl)amino]propyl]amino]-2-oxoethyl]-4-oxobutanoic acid. Ferric rhizobactin 1021 exists in solution predominantly in the Λ configuration, in an apparent equilibrium between a monomeric and a dimeric species.

Iron is essential for virtually all forms of life, and microorganisms have evolved elaborate and tightly regulated systems for its uptake. These systems are compatible with the extremely low solubility of polymeric ferric oxyhydroxides at neutral pH in an oxidizing atmosphere ($K_s = 10^{-38}$, $[Fe^{3+}] \approx 10^{-17}$ M) and the ability of iron ions to catalyze radical-producing reactions.[1,2] The extracellular components of these high-affinity iron acquisition systems are known as siderophores, Fe(III)-specific ligands that are excreted and, upon chelation, diffuse back to the cell surface and reenter the cell via outer membrane ferric siderophore receptors.[3] In host-dependent environments, microorganisms face the additional obstacle of iron-withholding mechanisms;[4] for endosymbiontic rhizobia, part of the life cycle involves invasion, growth, and differentiation within plant tissue.[5]

Rhizobium meliloti is an endosymbiont of *Medicago sativa* (alfalfa) and, like other rhizobia, induces nodule formation in the root cortex of its legume host.[5] Dinitrogen fixation is catalyzed by bacteroids in the nodules, and since both nitrogenase and leghemoglobin,[5] as well as regulatory proteins related to nitrogen fixation,[6] contain iron, a satisfactory supply of this element is essential.[7]

The hexadentate siderophore rhizobactin, a complexone type compound from *R. meliloti* DM-4, has been structurally characterized[8] and synthesized.[9] Siderophore-like compounds have also been isolated from other *Rhizobium* species.[10,11] Generally, however, the specifics of iron transport in rhizobia are not yet well understood. As a model for rhizobial iron transport, we have studied the high-affinity Fe(III) acquisition system of *R. meliloti* 1021. We report here the structure of rhizobactin 1021 (**1**), the siderophore of *R. meliloti* 1021. Rhizobactin 1021 is a novel citrate-based dihydroxamate siderophore that is asymmetric by virtue of the presence of two different acyl residues. One of these was identified as acetic acid and the other as (*E*)-2-decenoic acid, of which the latter is unique in a siderophore context. Several genes of this iron acquisition system have been cloned, including those for siderophore biosynthesis, transport, and regulatory elements.[12,13] The structure of rhizobactin 1021 is important, as its production may be related to the ability of *R. meliloti* 1021 to fix nitrogen; it was recently shown that many of the mutants defective in production of rhizobactin 1021 on a laboratory medium were also unable to efficiently fix nitrogen in planta.[14]

Experimental Section

Materials. Thenoyltrifluoroacetone (TTFA)[15] and (*E*)-2-octenoic acid were obtained from Aldrich. Bond Elut was from Analytichem Int. An enzyme kit for citrate determination was acquired from Boehringer Mannheim. Isobutyl methyl ketone (IBMK), 3-(dodecyldimethylammonium)propanesulfonic acid (DDAPS), and Chrome Azurol S (CAS) were purchased from Fluka. Desferal was a gift from Ciba-Geigy.

Microorganism. A previously described[12] mutant of *R. meliloti* 1021 (PRR 63), defective in a negative regulatory function for siderophore synthesis, was used for production of rhizobactin 1021. PRR 63 was

[†] Present address: Department of Biochemistry, 642 MRB, Center in Molecular Toxicology, Vanderbilt University, Nashville, TN 37232.
[‡] Present address: 35 Lathrop, Apt. 3B, Madison, WI 53705.
[§] Present address: Soil Microbial Systems Lab., Building 318, BARC-East, Beltsville, MD 20705.
[⊥] Present address: Simultec Ltd., Burgrain 37, CH-8706 Meilen/Zürich, Switzerland.
[∥] Present address: Microbiology Department, University College, Cork, Ireland.
* Phone (510) 642-7460. FAX (510) 643-5035.

(1) Bagg, A.; Neilands, J. B. *Microbiol. Rev.* **1987**, *51*, 509–518.
(2) Matzanke, B. F; Müller-Matzanke, G.; Raymond, K. N. In *Iron Carriers and Iron Proteins*; Loehr, T. M., Ed.; VCH Verlagsgesellschaft: Weinheim, 1989; pp 3–121.
(3) (a) Braun, V.; Winkelmann, G. *Prog. Clin. Biochem. Med.* **1988**, *5*, 67–99. (b) Hider, R. C. *Struct. Bonding (Berlin)* **1984**, *58*, 25–87. (c) Neilands, J. B. *Annu. Rev. Microbiol.* **1982**, *36*, 285–309.
(4) Weinberg, E. D. *Q. Rev. Biol.* **1989**, *64*, 261–290.
(5) (a) Djordjevic, M. A.; Gabriel, D. W.; Rolfe, B. G. *Annu. Rev. Phytopathol.* **1987**, *25*, 145–168. (b) Guerniot, M. L. *Dev. Plant Soil Sci.* **1991**, *130*, 199–209. (c) Verma, D. P. S.; Long, S. *Int. Rev. Cytol., Suppl.* **1983**, *14*, 211–245.
(6) (a) Hennecke, H. *Mol. Microbiol.* **1990**, *4*, 1621–1628. (b) Gilles-Gonzales, M. A.; Ditta, G. S.; Helinski, D. R. *Nature* **1991**, *350*, 170–172.
(7) (a) Nadler, K. D.; Johnston, A. W. B.; Chen, J.-W.; John, T. R. *J. Bacteriol.* **1990**, *172*, 670–677. (b) O'Hara, G. W.; Dilworth, M. J.; Boonkerd, N.; Parkpian, P. *New Phytol.* **1988**, *108*, 51–57. (c) Roessler, P. G.; Nadler, K. D. *J. Bacteriol.* **1982**, *149*, 1021–1026.
(8) Smith, M. J.; Shoolery, J. N.; Schwyn, B.; Holden, I.; Neilands, J. B. *J. Am. Chem. Soc.* **1985**, *107*, 1739–1743.
(9) Smith, M. J. *Tetrahedron Lett.* **1989**, *30*, 313–316.
(10) (a) Guerniot, M. L.; Meidl, E. J.; Plessner, O. *J. Bacteriol.* **1990**, *172*, 3298–3303. (b) Rioux, C. R.; Jordan, C. D.; Rattray, J. B. M. *Arch. Biochem. Biophys.* **1986**, *248*, 183–189.
(11) (a) Modi, M.; Shah, K. S.; Modi, V. V. *Arch. Mikrobiol.* **1985**, *141*, 156–158. (b) Patel, H. N.; Chakraborty, R. N.; Desai, S. B. *FEMS Microbiol. Lett.* **1988**, *56*, 131–134. (c) Skorupska, A.; Choma, A.; Derylo, M.; Lorkiewicz, Z. *Acta Biochim. Pol.* **1988**, *35*, 119–130.
(12) Gill, P. R., Jr.; Neilands, J. B. *Mol. Microbiol.* **1989**, *3*, 1183–1189.
(13) Reigh, G.; O'Connell, M. *J. Bacteriol.* **1993**, *175*, 94–102.
(14) Gill, P. R., Jr.; Barton, L. L.; Scoble, M. D.; Neilands, J. B. *Dev. Plant Soil Sci.* **1991**, *130*, 211–217.
(15) The abbreviations used are CAS, chrome azurol S; CD, circular dichroism; COSY, correlation spectroscopy; EPR, electron paramagnetic resonance; FAB MS, fast atom-bombardment mass spectrometry; IBMK, isobutyl methyl ketone; NMR, nuclear magnetic resonance; TTFA, thenoyltrifluoroacetone.

0002-7863/93/1515-3950$04.00/0

maintained on high-iron (200 μM) CAS agar,[16] with DDAPS equimolarly substituted for hexadecyltrimethylammonium bromide. The agar contained streptomycin (0.5 mg/mL) and neomycin (0.2 mg/mL).

Production and Purification. The medium for production of rhizobactin 1021 contained (in g/L) 4-morpholinepropanesulfonic acid (MOPS), 21; KOH, 6.5; sucrose, 10; deferrated Casamino acids, 20; fumaric acid, 2; histidine HCl·H_2O, 3.15; glutamic acid, 0.5; and yeast extract, 0.5. In addition, the medium contained 100 mL of 10X M9 salts[17] and biotin, 0.5 mg/L. The pH of the medium was maintained at 7.0. Rhizobactin 1021 was produced by incubating PRR 63 in 2.8-L Fernbach flasks containing 1 L of the medium on a rotary shaker at 30 °C. When cultures were in mid log phase (24–60 h), sterile cysteine and fumarate were added to 12.5 mM final concentration to enhance siderophore yields. After an additional 60 h, cells were killed by addition of sodium azide and pelleted by centrifugation, and the supernatant was saved for workup. The siderophore concentration at the time of harvest varied between 120 and 220 μM, as determined by the CAS assay for Fe(III) chelators.[16]

Each purification step was followed by one or more of the following analyses: the ferrozine reaction for ferrous iron,[18] the CAS assay, or UV/vis spectrophotometry, as applicable. In all handling of the free ligand, care was taken to keep pH above neutrality in order to avoid degradation (see below). Siderophores in the supernatant were adsorbed onto an XAD-4 resin overnight at 4 °C, at a ratio of 1 g of resin per 0.5 μmol of CAS activity as measured prior to azide addition. After filtration on a glass filter funnel, salts and debris were removed by washing with 3 volumes of cold water. Weakly adsorbed material was removed by washing with 1.25 volumes of prechilled aqueous methanol, once with 20% and 35% methanol and twice with 50% methanol, respectively. Desorption of rhizobactin 1021 was done in a large flask at 40–50 °C by 4–5 extractions during 15–20 min, each with approximately 1.5 resin volumes of methanol:2-propanol:H_2O (30:10:1).

The free ligand was then converted to its amber-colored ferric complex by addition of 0.1 M $FeCl_3$ in 15 mM HCl in 5% excess and neutralized with trimethylamine. Organic solvents were removed by rotary evaporation to near dryness with 2–3 additions of H_2O. The pH was maintained above neutrality by adding trimethylamine. A small amount of octanol was added to suppress excessive foaming during evaporation. After addition of H_2O to 250 mL, the solution was filtered to remove precipitates and extracted with ethyl acetate (1 volume). A ferrozine positive precipitate in the organic phase was back-extracted with H_2O. The aqueous fractions were combined, and ferric rhizobactin 1021 was transferred to an organic solvent by five extractions with 0.5 volumes of *n*-butanol. The combined extracts were concentrated at reduced pressure to 50 mM by the ferrozine assay and chromatographed on a 115- × 2.5-cm column with Sephadex LH-20 in a liquid phase of methanol or isobutyl alcohol:ethyl acetate:methanol (1:1:2).

Following solvent removal, ferric rhizobactin 1021 in water was lyophilized and taken up in a small volume of 10 mM triethylammonium carbonate, pH 7.5. Further purification was achieved by HPLC using a 250- × 10-mm semipreparative column with LiChrosorb RP-18, 7-μm particles (Merck) and a Hewlett-Packard HP 1090 liquid chromatograph equipped with a diode array detector. The solvent system consisted of (A) water and (B) 98.5% methanol, both containing 10 mM triethylammonium carbonate, pH 7.5. Samples were developed at a flowrate of 4 mL/min with the following elution profile (min, %B): 0–3, 55; 3–12.5, 55–65; 12.5–20, 65–80; 20–30, 80–100; 30–37.5, 100. The eluate was monitored at 400 nm, and five peaks were collected (Figure 1). After rotary evaporation of methanol, potassium phosphate was added to 10 mM, and fractions were lyophilized to remove triethylammonium carbonate. The purity of the five main fractions was checked on an analytical column, LiChrosorb RP-18, 5-μm particles (Merck), at a flowrate of 0.64 mL/min, using the same solvent system and gradient. All five fractions were saved for workup.

Ferric rhizobactin 1021 in potassium phosphate, pH 7.5, was deferrated by repeated vigorous mixing with 2.5% TTFA in IBMK in 50-mL Corex tubes. Phase separation was facilitated by centrifugation, and care was taken not to remove a precipitate at the interphase when the upper, organic layer was discarded. After deferration, the aqueous phase was washed with IMBK to remove traces of TTFA. Following lyophilization and resuspension in water, final purification was obtained by HPLC, using the same system as above and a liquid phase of (A) 1 mM potassium phosphate, pH 7.5, and (B) acetonitrile. Samples were developed at a flowrate of 4 mL/min with the following gradient, (time, %B): 0–5, 10; 5–25, 10–80; 25–29, 80. The eluate was monitored at 205 nm, and the main peak eluting at about 15.5 min was collected. Its purity was checked on an analytical column as above. To remove salts, rhizobactin 1021 was adsorbed onto 1-mL C18/OH Sep-Pak columns, washed with water, and eluated with methanol. Following lyophilization, the potassium salt of rhizobactin 1021 was stored dessicated at −20 °C.

Paper Electrophoresis. For high-voltage paper electrophoresis, a water-cooled flat bed apparatus connected to a Savant 0–2-kV constant voltage power supply was used. Samples were spotted onto Whatman No. 1 papers and the ionophoretic mobilities of compounds determined by electrophoresis at about 40 V/cm for 40–60 min in a buffer consisting of 33 mM phosphate, pH 6.5, or 8% acetic acid/2% formic acid, pH 1.9. Spots were detected by their color or by spraying with either alkaline ninhydrin or the CAS reagent.

Gel Filtration. The putative monomer and dimer of ferric rhizobactin 1021 were separated by gel-exclusion chromatography on a 1- × 65-cm column with Biogel P-2. The eluting solvent was 0.1 M Tris, pH 8.0, at a flowrate of 0.3 mL/min. For sizing, the column was standardized with the hydroxamate siderophores ferrichrome A, ferricrocin, and ferrioxamine B. Precise molecular weight determinations were made by FAB mass spectrometry.

Potentiometric Titration. Rhizobactin 1021, potassium salt (6.4 mg) was titrated with 0.1 N NaOH, which had been standardized against potassium hydrogen phthalate. Measurements were taken using a Metrohm 645 Multi-dosimat and a Corning 125 pH meter, calibrated with buffer standards prior to use. Traces were taken on a Kipp and Zonen BD 41 recorder.

Spectroscopy. Ultraviolet–visible (UV/vis) readings were taken on a Shimadzu UV-160 spectrophotometer, and spectra were recorded on a Cary 219 spectrophotometer. Circular dichroism (CD) measurements were made on an AVIV Model 60 DS CD spectropolarimeter.

NMR Spectroscopy. All spectra were obtained at the University of California, Berkeley, NMR Facility on a Bruker AM-400 spectrometer, operating at a 400.13-MHz proton frequency, equipped with an Aspect 3000 computer and digital phase switching hardware. Most spectra were processed on a Bruker X-32 data station.

Phase-sensitive double-quantum COSY spectra[19] were obtained, using the time-proportional phase incrementation (TPPI) method.[20] Each spectrum had 1024 complex t_2 data points and 512 t_1 data points; 32 scans per t_1 value were accumulated. The spectral width in both dimensions was 8.8 ppm. The data were zero filled to yield a final data matrix of 2048 real points in both dimensions, and resolution enhancement was achieved by processing with a $\pi/2$ phase-shifted sine bell function.

Two-dimensional decoupled ^1H–^{13}C correlation spectra were recorded in the inverse mode as described.[21] The spectral width was 9.6 ppm (3.8 Hz/pt) and 199 ppm (19.5 Hz/pt) in the proton and carbon dimension, respectively. The spectrum in Figure 3 was acquired with 1024 t_2 data points and 48 scans for each of 600 t_1 data points. Data were zero filled to give a final 1024 × 1024-point matrix, and both dimensions were processed with a $\pi/3$ phase-shifted cosine bell function.

Electronic Spin Resonance. EPR spectra of ferric complexes were obtained in frozen 0.1 M Tris·HCl, pH 8.0, at 8.5 K and a modulation frequency of 100 kHz on a Varian E-9 spectrophotometer at the Laboratory of Chemical Biodynamics, University of California, Berkeley. Other acquisition parameters were as described.[22] Fraction 1 (dimer) and fraction 2 (monomer) of ferric rhizobactin 1021 from gel-exclusion chromatography were collected and frozen immediately upon elution. Ferrichrome A in the same solvent was used as a reference. The concentration of ferric rhizobactin 1021, dimer, and ferrichrome A was 0.85 mM and that of ferric rhizobactin 1021, monomer, was 0.25 mM.

Analyses. Chemical analyses were done at the Unversity of California, Berkeley, Micro-analysis Facility. Amino acid analysis was performed with the amino acid analyzer at the Protein Structure Laboratory, School of Medicine, University of California, Davis. Gas chromatography–mass spectrometry (GC–MS), electronic impact (EI), and fast atom-bombardment (FAB) mass spectra were obtained at the University of California, Berkeley, Mass Spectrometry Facility.

Oxidative Degradation, Acid Hydrolysis, and Organic Acid Analysis. Hydroxamic acid residues were analyzed by the Csâky test[23] and by the periodate oxidation method.[24] In the former test, quantities of 15–30

(16) Schwyn, B.; Neilands, J. B. *Anal. Biochem.* **1987**, *160*, 47–56.
(17) Sambrook, J.; Fritsch, E. F.; Maniatis, T. *Molecular Cloning* 2nd ed.; Cold Spring Harbor Laboratory Press: Cold Spring Harbor, NY, 1989; p A3.
(18) Stookey, L. L. *Anal. Chem.* **1970**, *42*, 779–781.
(19) Rance, M.; Sørensen, O. W.; Bodenhausen, G.; Wagner, G.; Ernst, R. R.; Wüthrich, K. *Biochem. Biophys. Res. Commun.* **1983**, *117*, 479–485.
(20) Marion, D.; Wüthrich, K. *Biochem. Biophys. Res. Commun.* **1983**, *113*, 967–974.
(21) (a) Bax, A.; Morris, G. J. *J. Magn. Reson.* **1981**, *42*, 501–505. (b) Bax, A.; Subramanian, S. J. *J. Magn. Reson.* **1986**, *67*, 565–569.
(22) Barclay, S. J.; Huynh, B. H.; Raymond, K. N. *Inorg. Chem.* **1984**, *23*, 2011–2018.

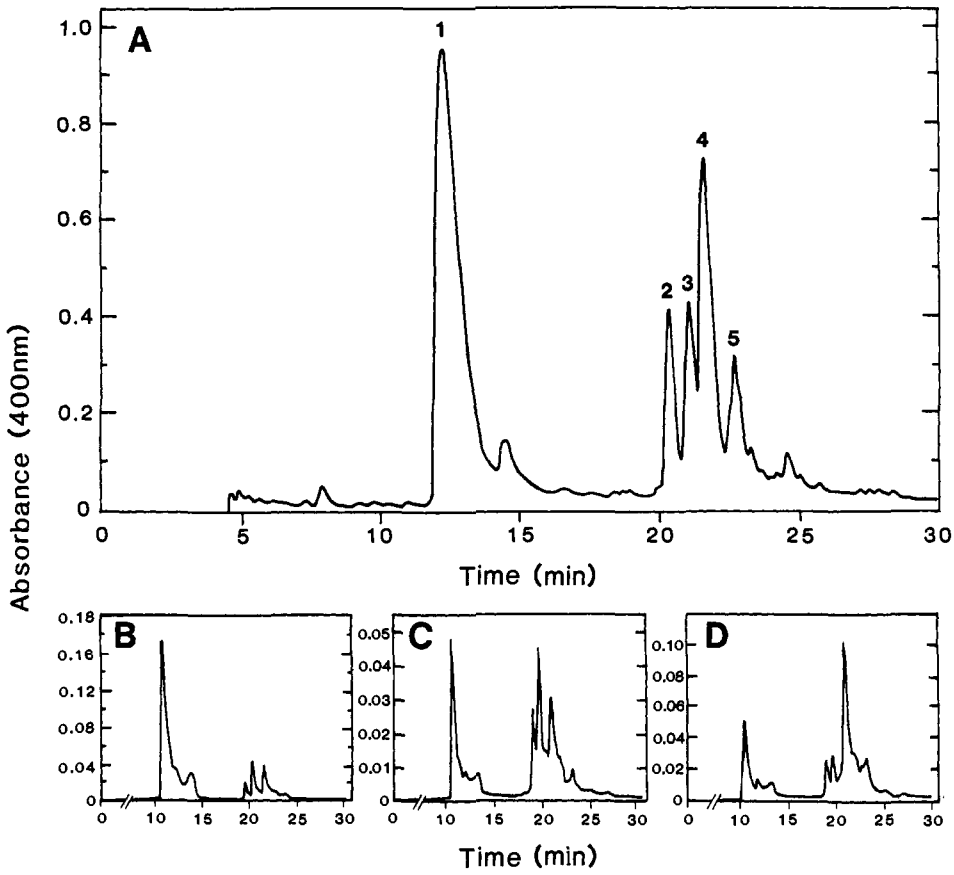

Figure 1. (A) Chromatogram from semipreparative HPLC purification of ferric rhizobactin 1021. (B–D) Analytical HPLC trace of material from peaks 1, 3, and 4, respectively. The appearance in each case of several peaks with overall similarity to the initial chromatogram indicates multiple, interconverting forms of the ferric complex.

nmol of rhizobactin 1021, 5–30 nmol of deferri-ferrioxamine B, and 1.5–30 nmol of hydroxylamine·HCl were used. The latter analysis was performed with 0.2 μmol of rhizobactin 1021, deferri-ferrioxamine B, and deferri-ferrichrome A.

For determination of the tricarboxylic acid residue, 90 μg of rhizobactin 1021 was hydrolyzed in vacuo with 6 N HCl at 110 °C for 20 h. Excess mineral acid was removed by several evaporations under reduced pressure. The residue was taken up in H_2O, and citric acid was determined by an NADH-coupled enzyme assay kit containing citrate lyase, malate dehydrogenase, L-lactic acid dehydrogenase, and NADH, as specified by the manufacturer.[25]

For identification of the two hydroxamic acid acyl groups, 0.7 mg of rhizobactin 1021 was oxidized in 1.0 mL of a 0.05% periodic acid solution, and the carboxylic acids were extracted into ether after acidification with HCl. The solution was evaporated to dryness and the residue taken up in CD_3OD, after which the ^1H NMR spectrum was recorded. The ^1H NMR spectrum of (*E*)-2-octenoic acid was obtained as a reference. The solution was again evaporated to dryness, dissolved in methanol, and analyzed with GC–MS. A 0.4-mg sample was analyzed by EI directly following periodate oxidation, after transferring the carboxylic acids to methanol without drying.

Hydrolysis of ferric rhizobactin 1021 and rhizobactin 1021 with 47% HI as above was used to identify the amine function. Samples were extracted with ether, and the aqueous phase was evaporated to dryness repeatedly to remove excess HI. Residues were dissolved in a minimal volume of water and analyzed by paper electrophoresis at pH 1.9 with diaminopropane, diaminobutane, and diaminopentane as references.

Results and Discussion

Isolation and Characteristics. Rhizobactin 1021 was isolated mainly as the ferric complex, since the free ligand was subject to rapid degradation. In unbuffered aqueous solution, the degradation proceeded quantitatively overnight. This was identified by FAB as a loss of water, m/z from 531 to 513 for $[MH]^+$, with a concomitant transition from an anionic to a neutral species, consistent with imide formation. Rapid formation at low pH of very stable five-membered cyclic imides by amidated citrate-based siderophores has been noted during both purification[26,27,28b] and synthesis.[29] This facile proton-catalyzed formation of imide bonds, and their stability under hydrolytic conditions, likely explain the low yields from the various chemical tests in which these conditions were encountered. Very low yields, attributed to stable cyclic imides, were also reported for amino acid analysis following acid hydrolysis of staphyloferrin A.[26] However, purification of ferric rhizobactin 1021 was a concession to stability over practicability, as the ferric complex was found to exist in several forms. This was evident in all chromatography steps as multiple, amber, ferrozine-positive bands and was especially striking by HPLC. The starting material separated into five, major, ferrozine-positive fractions with a λ_{max} at 399 nm. Upon reinjection of an isolated peak, the original chromatographic pattern was essentially obtained (Figure 1). Virtually identical UV/vis and FAB mass spectra ($[MH]^+$, m/z 584) suggested the presence of one ligand. This was confirmed after deferration on material from three fractions by identical HPLC retention (15.5 min), FAB MS ($[MH]^+$, m/z 531), and, save for minor contaminants, ^1H NMR spectra.

Ferric rhizobactin 1021 resisted attempts at crystallization and was obtained as a fluffy, brown powder with a somewhat unpleasant odor. By paper electrophoresis at pH 6.5, ferric

(23) Gillam, A. H.; Lewis, A. G.; Andersen, R. J. *Anal. Chem.* **1981**, *53*, 841–844.
(24) Emery, T. F.; Neilands, J. B. *J. Org. Chem.* **1962**, *27*, 1075–1076.
(25) Möllering, H. In *Methods of Enzymatic Analysis*, 3rd ed.; Bergmeyer, H. U., Ed.; VCH Verlagsgesellschaft: Weinheim, 1985; Vol. 7, pp 2–12.
(26) Konetschny-Rapp, S.; Jung, G.; Meiwes, J.; Zähner, H. *Eur. J. Biochem.* **1990**, *191*, 65–74.
(27) Mullis, K. B.; Pollack, J. R.; Neilands, J. B. *Biochemistry* **1971**, *10*, 4894–4898.
(28) (a) Drechsel, H.; Metzger, J.; Jung, G.; Boelaert, J. R.; Winkelmann, G. *Biol. Met.* **1991**, *4*, 238–243. (b) Drechsel, H.; Jung, G.; Winkelmann, G. *Biol. Met.* **1992**, *5*, 141–148.
(29) Lee, B. H.; Miller, M. J. *J. Org. Chem.* **1983**, *48*, 24–31.

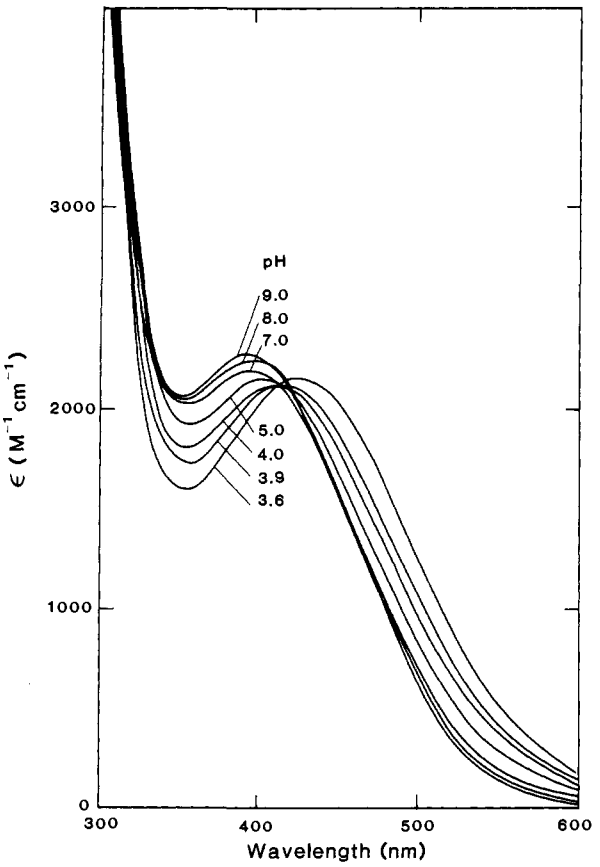

Figure 2. Visible spectrum of ferric rhizobactin 1021 in aqueous medium as a function of pH.

rhizobactin 1021 moved slightly faster than the dimethyl ester of ferrichrome A, indicating a monoanionic charge. In neutral aqueous solution, the compound had a golden-brown color. The visible absorption spectrum showed a broad metal-to-ligand charge-transfer band with λ_{max} = 399 nm (ϵ = 2.2 × 10^3 M^{-1} cm^{-1}). Unlike ferric trihydroxamate siderophores, the spectrum was sensitive to $[H]^+$ (Figure 2) and qualitatively very similar to the spectra of ferric schizokinen (**3**)[30] and ferric aerobactin,[31] two citrate-based dihydroxamate siderophores. As the pH was depressed from 7 to 3.6, the spectrum shifted to the red, through an isosbestic point near 412 nm to a slightly higher maximum at 426 nm. As for the ferric complexes of schizokinen[30b] and aerobactin,[31] the pH dependence of the spectrum probably corresponded to protonation of the hydroxyl group of the citric acid moiety. At pH values below 3.6, the complex precipitated within 15 min of preparation, and at pH 3.6 and 3.9, some precipitation was noted after about an hour.

Rhizobactin 1021 of ≥95% purity was obtained in approximately 10% total yield, based on the concentration of iron chelators in the fermentation broth. The compound was very hygroscopic and probably owed its tan color to a rather broad peak in the UV region, tapering off at about 300 nm from a maximum at 205 nm (ϵ = 2.9 × 10^4 M^{-1} cm^{-1}). Rhizobactin 1021 had a negative ninhydrin reaction, and no evidence for amino acids was found in samples hydrolyzed with either HCl or HI. Furthermore, the ^1H NMR spectrum indicated an absence of amino acids, as it lacked peaks in the region for C_α protons (see below).

Two methods were used for hydroxamate determination, and rhizobactin 1021 was positive by both the Csâky method and periodate oxidation.[32] Potentiometric titration yielded a buffer region around pH 9.0 with a neutral equivalent of 284 (potassium salt). This is consistent with the presence of two hydroxamic acid equivalents, for which pK_a's of about 9 are typical.[33]

Structure of Rhizobactin 1021. Mass Spectrometry and Elemental Analysis. The structure of rhizobactin 1021 (**1**) was afforded by a combination of mass spectrometric, NMR, and degradation techniques.

FAB MS of rhizobactin 1021 revealed peaks at m/z 531 (100), 553 (8), and 515 (7) for $[MH]^+$, $[MNa]^+$ and $[MH - O]^+$, respectively.[34] The accurate mass for the $[MH]^+$ ion was determined by high-resolution FAB MS as being 531.3025, consistent with two elemental compositions containing both nitrogen and oxygen; $C_{24}H_{43}N_4O_9$ (Δ0.5 mmu) and $C_{36}H_{39}N_2O_2$ (Δ1.4 mmu). On the basis of chemical and nuclear magnetic resonance evidence (see below), the latter could be excluded. High-resolution FAB MS of ferric rhizobactin 1021 and its sodium adduct yielded molecular ions at m/z 584.2149 for $[MHFe - 3H]^+$, and 606.1975 for $[MFeNa - 3H]^+$, consistent with $C_{24}H_{40}N_4O_9Fe$ (Δ0.4 mmu) and $C_{24}H_{39}N_4O_9FeNa$ (Δ1.1 mmu), respectively. The presence of a molecular ion for the ferric complex 53 mass units higher than the free ligand indicated a metal-to-ligand ratio of 1. Elemental analysis of the amorphous, fluffy powder of ferric rhizobactin 1021 gave inconsistent results. However, there was no analytical evidence for sulfur, and the O:N ratio was about 5:2.

NMR Spectroscopy. The ^1H NMR spectral values of rhizobactin 1021 are summarized in Table I. Signals were generally broad, possibly owing to iron contamination but more probably to intermolecular interactions. Spectra showed extremely broad lines in D_2O or $CDCl_3$. Integration gave 36 protons, of which several were poorly resolved. The ^1H NMR spectrum of nondeuterated rhizobactin 1021 in DMSO-d_6 showed an additional two signals in the amide region (Table I) and one broad peak at 10.5 ppm, presumably from hydroxyl group(s).

A DQ COSY spectrum readily allowed the identification of five spin systems. One was assigned to the methyl singlet from the acetyl hydroxamate group. Two essentially degenerate pairs constituted the remaining four. One pair was composed of the two diastereotopic methylenes from the citrate moiety, while the other pair belonged to the 1-amino-3-hydroxyamino propane methylenes. The remaining proton signals (H-1–9) could not be unambiguously assigned to spin system(s), as the four methylene signals in the envelope at 1.3 ppm (H-2–5) were insufficiently resolved. However, the degeneracy of their chemical shifts strongly suggested a nearly identical chemical environment. By the presence of only one alkyl methyl group and the near identity of the subspectrum of H-1–9 by both ^1H and ^{13}C NMR with the chemical shifts of octenoic acid and nonenoic acid,[35] it was suspected that the envelope methylenes were contained within one spin system, making a total of six isolated spin systems. This hypothesis was confirmed by the extraction of (*E*)-2-decenoic acid from periodate-oxidized rhizobactin 1021 (see below).

The broad-band decoupled ^{13}C spectrum (Table II) showed 23 resolved signals, the multiplicity of which were determined by the DEPT experiment. However, of the four carbonyl signals, the peak at 172.9 ppm, which had an intensity more than twice

(30) (a) Byers, B. R.; Powell, M. V.; Lankford, C. E. *J. Bacteriol.* **1967**, *93*, 286–294. (b) Plowman, J. E.; Loehr, T. M.; Goldman, S. J.; Sanders-Loehr, J. *J. Inorg. Biochem.* **1984**, *20*, 183–197.

(31) Harris, W. R.; Carrano, C. J.; Raymond, K. N. *J. Am. Chem. Soc.* **1979**, *101*, 2722–2727.

(32) Compared to trihydroxamate siderophores, yields were lower than expected for the proposed structure by factors of 3–6 and 1.5 for the two methods, respectively. This was attributed to acid catalyzed formation of hydrolytically stable cyclic imides.

(33) Sillén, L. G.; Martell, A. E. *Stability Constants*; The Chemical Society, Burlington House: London, 1964; Special Publication No. 17, pp 727–730.

(34) A characteristic loss of the hydroxyamino oxygen has previously been observed by mass spectrometry of hydroxamic acid siderophores. (a) Akers, H. A.; Atkin, C. L.; Neilands, J. B. *Org. Mass Spectrom.* **1975**, *10*, 259–262. (b) Dell, A.; Hider, R. C.; Barber, M.; Bordoli, R. S.; Segdwick, R. D.; Tyler, A. N.; Neilands, J. B. *Biom. Mass Spectrom.* **1982**, *9*, 158–161. (c) Deml, G.; Voges, K.; Jung, G.; Winkelmann, G. *FEBS Lett.* **1984**, *173*, 53–57. (d) Nishio, T.; Tanaka, N.; Hiratake, J.; Katsube, Y.; Ishida, Y.; Oda, J. *J. Am. Chem. Soc.* **1988**, *110*, 8733–8734.

(35) (a) Breitmaier, E.; Haas, G.; Voelter, W. *Atlas of Carbon-13 NMR Data*; Heyden: London, 1979; Vol. 1–2. (b) *Handbook of Proton-NMR Spectra and Data*; Shin-ichi, S., Ed.; Academic Press: Tokyo, 1985; Vol. 3, p 205.

Table I. ^{1}H Chemical Shifts (δ, ppm) and Coupling Constants (J, Hz) of Rhizobactin 1021 (**1**), (*E*)-2-Decenoic Acid (**2**),[c] (*E*)-2-Octenoic Acid (**4**),[d] Schizokinen (**3**),[e] and Two Diastereotopic Citrate CH_2 Groups from Staphyloferrin A (**5**)[f]

position	group	1[a]	1[b]	2	4	3	5
H-1	CH_3	0.90 (t) ($^3J_2$ = 6.9)	0.86	0.90	0.90		
H-2	CH_2	1.31 (m)	1.26	1.33	1.32		
H-3	CH_2	1.31 (m)	1.26	1.33	1.32		
H-4	CH_2	1.31 (m)	1.26	1.33	1.47		
H-5	CH_2	1.31 (m)	1.26	1.33	2.21 ($^3J_6$ = 7.2, $^4J_7$ = 1.2)		
H-6	CH_2	1.48 (m)	1.40	1.46	6.92, 6.96 ($^3J_5$ = 7.1, $^3J_7$ = 15.6)		
H-7	CH_2	2.27 (dt) ($^3J_8$ = 6.9)	2.17 ($^3J_8$ = 6.9)	2.20 ($^3J_8$ = 7.2, $^4J_9$ = 1.2)	5.78 ($^3J_6$ = 15.6, $^4J_5$ = 1.5)		
H-8	CH_2–*CH*	6.86, 6.89 (dt) ($^3J_7$ = 6.8, $^3J_9$ = 15.5)	6.65, 6.69 ($^3J_7$ = 7.0, $^3J_9$ = 15.4)	6.88, 6.91 ($^3J_7$ = 7.1, $^3J_9$ = 15.5)			
H-9	*CH*–C(=O)	6.61 (d) ($^3J_8$ = 15.5)	6.52 ($^3J_8$ = 14.6)	5.78 ($^3J_8$ = 15.5, $^4J_7$ = 1.2)			
H-1′	C(=O)–*CH*$_3$	2.15 (s)	1.97			2.12	
H-1″	*CH*$_2$–N(OH)–C(=O)	3.74[g] (t)	3.57[g]				
H-2″	CH_2	1.85 (m)	1.63				
H-3″	*CH*$_2$–NH–C(=O)	3.22 (m)	3.02				
H-4″	*NH*–C(=O)		7.88				
H-1‴	*CH*$_2$–N(OH)–C(=O)	3.67 (t)	3.51			3.68	
H-2‴	CH_2	1.85 (m)	1.63			1.83	
H-3‴	*CH*$_2$–NH–C(=O)	3.22 (m)	3.02			3.23	
H-4‴	*NH*–C(=O)		7.82				
H-2⁗A	(HO)C–H*CH*–C(=O)	2.578, 2.614[h] (d) (^2J = 14.4)	2.337 (^2J = 3.5)			2.67	2.709, 2.747 (^2J = 15.0)
H-2⁗B	(HO)C–*HC*H–C(=O)	2.671, 2.707 (d) (^2J = 14.3)	2.345 (^2J = 3.5)			2.67	2.774, 2.812 (^2J = 15.0)
H-5⁗A	(HO)C–H*CH*–C(=O)	2.578, 2.614 (d) (^2J = 14.4)	2.337 (^2J = 3.5)			2.67	2.733, 2.774 (^2J = 16.0)
H-5⁗B	(HO)C–*HC*H–C(=O)	2.677, 2.713 (d) (^2J = 14.5)	2.337 (^2J = 3.5)			2.67	2.929, 2.969 (^2J = 16.0)

[a] Solvent, D_2O:CD_3OD (2:3) with 20 mM K_2HPO_4, pH 7.5. Chemical shifts are referred to internal DSS at 0.028 ppm. [b] Solvent, DMSO-d_6. Nondeuterated rhizobactin 1021. Chemical shifts are referred to internal DSS at 0.000 ppm. [c] Ether extractable acid from periodate oxidation of rhizobactin 1021. Solvent, CD_3OD. [d] Solvent, CD_3OD. [e] From ref 27. Solvent, D_2O. [f] From ref 26. Solvent, CD_3OD:D_2O (2:3). [g,h] The absolute position of spin systems 1″–4″ and 1‴–4‴ and those of 2⁗ and 5⁗, respectively, may be interchanged.

Table II. ^{13}C Chemical Shifts (δ, ppm) of Rhizobactin 1021

position	group	1[a]
C-1	CH_3	14.03
C-2	CH_2	22.92
C-3	CH_2	32.07[c]
C-4	CH_2	29.33[c]
C-5	CH_2	29.29[c]
C-6	CH_2	28.48
C-7	CH_2	32.75
C-8	*CH*=CH	149.02
C-9	CH=*CH*	119.29
C-10	C(=O)	168.40[d]
C-1′	*CH*$_3$–C(=O)	19.90
C-2′	CH$_3$–*C*(=*O*)	173.92[d]
C-1″ [b]	C*H*$_2$–*N*(OH)–C(=O)	46.70
C-2″	CH_2	26.76
C-3″	*CH*$_2$–NH–C(=O)	37.66
C-1‴	*CH*$_2$–N(OH)–C(=O)	46.30
C-2‴	CH_2	26.68
C-3‴	*CH*$_2$–NH–C(=O)	37.31
C-1⁗	C(=O)	172.88
C-2⁗	CH_2	45.18[e]
C-3⁗	C	75.63
C-4⁗	C(=O)	179.41
C-5⁗	CH_2	45.26[e]
C-6⁗	C(=O)	172.88

[a] Spectrum obtained in D_2O:CD_3OD (2:3) with 20 mM K_2HPO_4, pH 7.5 and referred to internal dioxane at 67.40 ppm. [b] The absolute position of spin systems 1″–3″ and 1‴–3‴ may be interchanged. [c–e] Chemical shifts with the same superscript may be transposed.

that of any other, was assigned to the two distal carbonyls of citrate. Accordingly, rhizobactin 1021 contained 24 carbons, consistent with the elemental composition obtained by high-resolution FAB MS.

A striking feature of both the ^{1}H and ^{13}C spectra, especially prominent in the ^{1}H–^{13}C correlation spectrum (Figure 3), was the presence of several virtually overlapping peaks which indicated some degree of symmetry in rhizobactin 1021. The symmetrical units were determined to belong to the two pairs of degenerate spins systems mentioned above, namely, the two citrate methylenes and the three methylene groups from the two 1-amino-3-(hydroxyamino)propane moieties.

Subunits. The presence of a citrate moiety in rhizobactin 1021 was indicated by the above mentioned UV/vis spectral similarity to ferric schizokinen and ferric aerobactin. The characteristic doublet of doublets at 2.6 and 2.7 ppm in the ^{1}H NMR spectrum (Table I), which had the appearance of two partial AX groups ($\Delta\delta/J$ = 3.1 Hz), was assigned to the two diastereotopic methylenes of the citric acid residue. From these, a maximum of eight signals are theoretically possible. Only six were observed, as the high-field doublets were completely degenerate in all solvents tried. Values for the geminal coupling constants of 14.4 and 14.5 Hz correspond well to published values for staphyloferrin A, a chiral citrate-based siderophore.[26] In the ^{13}C spectrum, the chemical shifts of two methylenes and the quaternary carbon were nearly identical to those of citrate and citrate derivatives.[26,35a] Furthermore, citric acid was found in 54% yield in a HCl hydrolysate of rhizobactin 1021 by the NADH coupled enzyme assay.

Based on partial identity of the ^{1}H spectra of rhizobactin 1021 and schizokinen[27,30b,36] (Table I), it was suspected that the hydroxylamine moieties belonged to 1-amino-3-(hydroxyamino)-propane. By paper electrophoresis of reductively hydrolyzed rhizobactin 1021, the major spot comigrated with diaminopropane, slightly faster than either diaminobutane or diaminopentane, confirming the presence of the three carbon diamine. Two weak, closely spaced spots with approximately half the ionophoretic mobility presumably represented the two ring-closed imide forms of rhizobactin 1021.

One of the two acyl groups required for hydroxamic acid formation was determined to be acetic acid. The ^{1}H NMR methyl

(36) Simpson, F. B.; Neilands, J. B. *J. Phycol.* **1976**, *12*, 44–48.

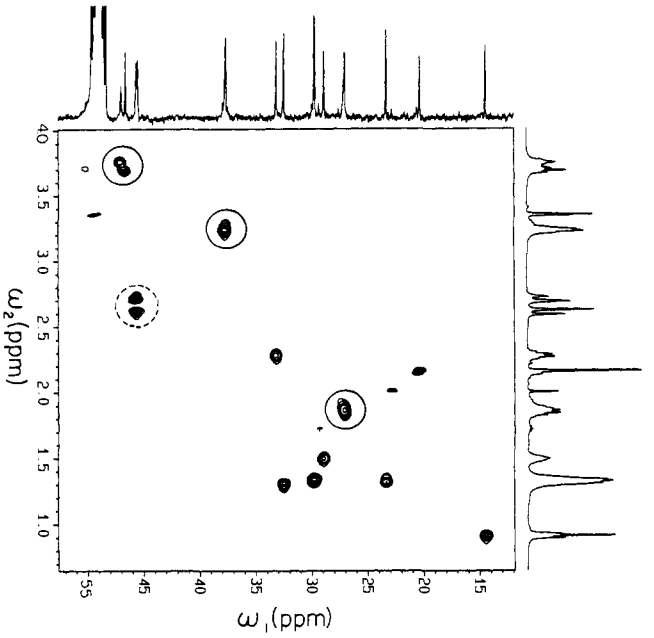

Figure 3. Alkyl region of the ^1H–^{13}C correlation spectrum of rhizobactin 1021. To illustrate the partial symmetry of the molecule, the methylene signals from the two 1-amino-3-(hydroxyamino)propane moieties and the two diastereotopic citrate methylene groups are circled with solid and dashed lines, respectively.

singlet at 2.15 ppm in D_2O and 1.97 ppm in DMSO-d_6 is characteristic of acetyl hydroxamates.[37] Acetic acid was also identified by EI as an m/z 60 peak in an ether extract of periodate-treated rhizobactin 1021.

NMR data indicated that the second acyl group in rhizobactin 1021 was derived from (*E*)-2-decenoic acid (**2**) (Table I). The ^1H and ^{13}C chemical shift values, the characteristic appearance as a doublet of triplets and a doublet, and the ^1H coupling constants indicated that the vinyl protons at 6.6 and 6.9 ppm were positioned trans next to a carbonyl group. After periodate oxidation, which is known to liberate the acyl moiety from hydroxamic acids,[24] peaks with chemical shifts and coupling constants essentially identical to those of (*E*)-2-octenoic acid were identified by ^1H NMR (Table I). Notable is the large chemical shift change ($\Delta\delta$ = 0.83 ppm) of the vinyl proton H-9, α to the carbonyl group, upon liberation of the acid by periodate oxidation. The number of methylene groups (4) in the envelope corresponded to the expected value for (*E*)-2-decenoic acid. From periodate-treated and ether-extracted rhizobactin 1021, a peak with m/z 170 (24), the expected $[M]^+$ ion for decenoic acid, was identified by GC–MS.[38]

Ferric Rhizobactin 1021. By CD spectroscopy of ferric rhizobactin 1021 at neutral pH, four peaks were observed in the visible region: 459 (–0.06), 405 (0.16), 349 (–0.54), 310 (0.28) nm ($\Delta\epsilon$). Correlation of X-ray diffraction data to CD spectra of ferric siderophores and resolved model complexes has allowed a relation to be drawn between the sign of the peak, which corresponds to the charge-transfer band in the electronic spectrum (Figure 2), and absolute configuration.[2,39] The CD spectrum of ferric rhizobactin 1021 was qualitatively similar to those ferric siderophores that have been shown to possess the Λ configuration. Consequently, we conclude that the dominant optical isomer of ferric rhizobactin 1021 in solution also has the Λ configuration. However, the amplitude of this peak is about 1 order of magnitude lower than those for ferric siderophores of the trihydroxamate type.[2,39] Similar observations were also made for ferric aerobactin.[31] It is unclear if this difference is due to different coordination spheres or to a Λ–Δ equilibrium with one optical isomer in slight excess. Rhizobactin 1021 may be either *R* or *S* with respect to the quaternary carbon of the citrate moiety. Its ferric complex in the Λ form can theoretically form eight different geometric isomers. Space filling models indicate that only Λ-*N*-cis-trans and Λ-*N*-cis-cis are possible, using the nomenclature for ferric aerobactin.[31] However, the former appeared to be somewhat, and the latter severely, constrained. A model which would allow strain-free octahedral coordination and be compatible with our physicochemical data is a binuclear complex. A binuclear complex could, according to CPK models, easily be formed by the alignment of two monomers and mutual donation of a hydroxamate-bearing side chain. The resulting dimer would thus be hexacoordinate and expected to show the same optical properties as the monomer.

Upon gel exclusion chromatography of ferric rhizobactin 1021, the golden-brown solution separated into two bands, the intensity of which varied with the chromatographic conditions. The slower moving band (monomer) appeared gradually and increased in intensity with increasing column length and temperature, concomitant with a decrease in intensity of the faster moving band (dimer), suggesting an equilibrium between the two forms. A zone of weak absorptivity separated the two bands. The average size of the faster moving band was 1100, in good agreement with the theoretical and mass spectral value of 1166 for dimeric ferric rhizobactin 1021. The slower moving band eluted at a volume corresponding to a size of 870, 1.5 times the mass spectral monomeric value. All FAB mass spectra of ferric rhizobactin 1021 showed peaks at m/z 584 and 1167, which were attributed to $[MFe - 3H + H]^+$ and $[2(MFe - 3H) + H]^+$, respectively.

The EPR spectra of frozen solutions of ferrichrome A and the proposed monomer and dimer of ferric rhizobactin 1021 were recorded. All three complexes were EPR active, with a resonance at $g = 4.3$, characteristic of high-spin octahedral ferric iron (Figure 4). This was previously observed for the siderophores ferrichrome A[40] and ferric rhodotorulic acid.[22] The spectra of ferrichrome A and ferric rhizobactin 1021, monomer, were essentially identical, showing sharp peaks with ΔH = 62 G and 40 G, respectively. However, the peak of ferric rhizobactin 1021, dimer, was significantly broadened, ΔH = 192 G. The peak broadening, accompanied by a decrease in intensity, could be explained by dipolar coupling between the two ferric ions in the proposed dimer. It has been calculated that for high-spin Fe(III), dipole–dipole interactions are significant at distances of less than 9 Å,[41] and molecular models suggest that in the proposed dimeric structure the metal–metal distance would be between 6 and 8 Å. In a study of the dihydroxamate siderophore rhodotorulic acid, which forms a binuclear complex, model compounds were used to vary the distance between the ferric ions from 12 to 5 Å by a successive shortening of the ligand backbone. In complexes in which the backbone brought the ferric ions closer than about 8.5 Å, significant line broadening was observed.[22]

These data support our proposed model of ferric rhizobactin 1021 in solution as an equilibrium between a monomeric and a dimeric species. The existence of a dimer may be explained by the strain of the ligand backbone upon chelation, which could reduce the free energy difference betwee the two species. An equilibrium of monomeric and dimeric ferric rhizobactin 1021 would also explain the multiple, interchangeable bands observed by HPLC. The dimer could, according to models, adopt several

(37) (a) Gibson, F.; Magrath, D. I. *Biochim. Biophys. Acta* **1969**, *192*, 175–184. (b) Frederick, C. B.; Bentley, M. D. *Biochemistry* **1981**, *20*, 2436–2438. (c) Jalal, M. A. F.; van der Helm, D. *Biol. Met.* **1989**, *2*, 11–17. (d) Keller-Schierlein, W. *Helv. Chim. Acta* **1963**, *46*, 1920–1929. (e) Keller-Schierlein, W.; Diekmann, H. *Helv. Chim. Acta* **1970**, *53*, 2035–2044. (f) Yang, C.-C.; Leong, J. *J. Bacteriol.* **1982**, *149*, 381–383.

(38) Other peaks observed at m/z: 115 (8) $C_6H_{11}O_2$; 101 (14) $C_5H_9O_2$; 87 (64) $C_4H_7O_2$; 73 (77) $C_3H_5O_2$; 85 (6) C_6H_{13}; 71 (17) C_5H_{11}; 57 (24) C_4H_9; and 86 (29) $C_4H_6O_2$.

(39) van der Helm, D.; Jalal, M. A. F.; Hossain, M. B. In *Iron Transport in Microbes, Plants and Animals*; Winkelmann, G., van der Helm, D.; Neilands, J. B., Eds.; VCH Verlagsgesellschaft: Weinheim, 1987; pp 135–165.

(40) Wickman, H. H.; Klein, M. P.; Shirley, D. A. *J. Chem. Phys.* **1965**, *42*, 2113–2117.

(41) Aasa, R.; Malmström, B. G.; Saltman, P.; Vänngård, T. *Biochim. Biophys. Acta* **1963**, *75*, 203–222.

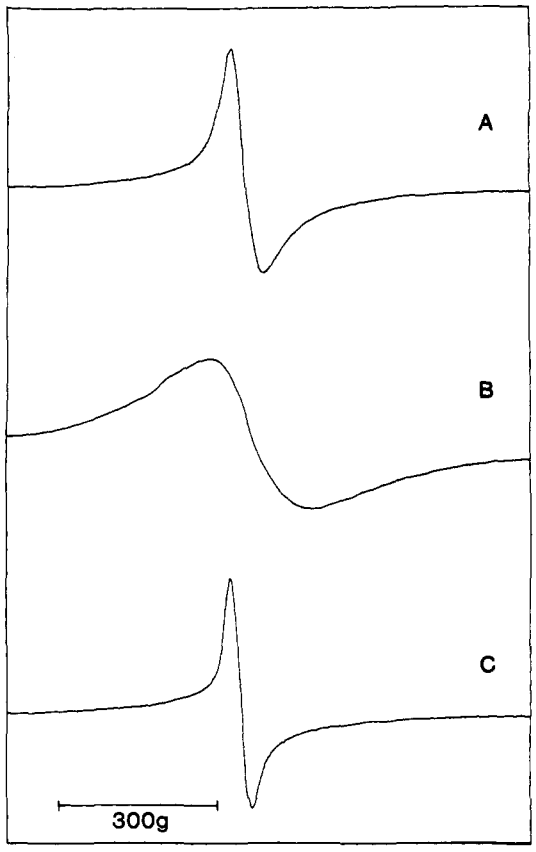

Figure 4. EPR spectra of (A) ferrichrome A, (B) ferric rhizobactin 1021, dimer, and (C) ferric rhizobactin 1021, monomer. Conditions were as described in ref 22.

configurations that may display different chromatographic behavior.

Concluding Remarks. Rhizobactin 1021[42] is structurally similar to the citrate-based dihydroxamate siderophores schizokinen,[27] aerobactin,[37a] and arthrobactin,[43] all of which have been synthesized.[29,44] The citrate moiety in these siderophores is symmetrically substituted, whereas two different carboxylic acids acylate the hydroxylamine residues in rhizobactin 1021. Staphyloferrin A[26] and rhizoferrin,[28] two recently characterized citrate-based siderophores, are likewise chiral. These siderophores do not, however, contain hydroxamic acid functions but were proposed to coordinate Fe(III) via the two citric acid moieties amide bonded to ornithine and diaminobutane, respectively.

The presence in rhizobactin 1021 of a fatty acid residue would explain its highly amphiphilic properties, manifested by solubility inboth H_2O and a range of organic solvents. The (*E*)-2-decenoic acid residue has never been positively identified as a siderophore constituent and is possibly new as a microbial metabolite. It has previously been identified in the occipital gland secretion from the Bactrian camel[45] and in the royal jelly and the mandibular glands of the honey bee.[46] Long-chain fatty acids in siderophores have been found in mycobactins from mycobacteria,[47] and

Scheme I. Structure of (**1**) rhizobactin 1021, (**2**) decenoic acid, and (**3**) schizokinen

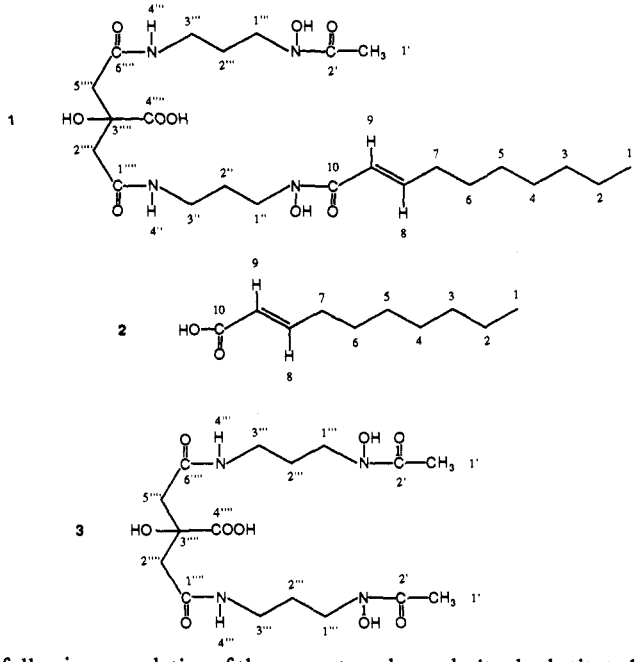

following completion of the present work, a palmitoyl substituted coprogen was reported from *Trichoderma*.[48] The significance of the decenoic acid residue in rhizobactin 1021, if any, is unclear, although it is conceivable that its surfactant properties may play a role in the membrane translocation of the ferric complex by making the molecule more mobile.

The one detail of the structure of rhizobactin 1021 we have not elucidated is the absolute configuration at the quaternary carbon of the citrate moiety. This probably warrants a separate investigation, which should include determination of the configuration of N^2-citryl-N^6-acetyl-N^6-hydroxylysine, an intermediate in the biosynthesis of aerobactin.[49] Aerobactin appears to confer virulence to enterobacterial strains, possibly by its ability to efficiently remove transferrin bound iron,[50] and we may note that both the pathogenic aerobactin producing enterobacterial strains and the symbiont *R. meliloti* must obtain necessary iron from their respective hosts. It may thus appear that these siderophores with relatively modest formation constants[31] are efficient in overcoming host-imposed nutritional immunity.

Acknowledgment. We gratefully acknowledge the use of equipment in the laboratory of Dr. R. D. Cole, Dr. V. Yachandra in the laboratory, Dr. M. P. Klein for obtaining EPR spectra, and the technical assistance of Dr. E. Alvarado and the staff at the University of California, Berkeley, Mass Spectrometry Facility. This work was supported in part by grants AI04156 and CRCR-1-1633 from the NIH and USDA, respectively.

Note Added in Proof: The recent work on the citrate–hydroxamate siderophores from the bacterium *Nannocystis exedens* has come to our attention [Kunze, B.; Trowitzsch-Kienast, W.; Höfle, G.; Reichenbach, H. *J. Antibiot.* **1992**, *45*, 147–150. Bergeron, R. J.; Phanstiel, O., IV *J. Org. Chem.* **1992**, *57*, 7140–7143]. It is clear that nannochelin B is chiral by virtue of the presence of one free and one carboxymethyl substituent in the amide-linked side chains attached to the terminal carboxyl groups of the citrate moiety.

(42) A preliminary account of the characteristics of rhizobactin 1021 has been published (Schwyn, B.; Neilands, J. B. *Comments Agric. Food Chem.* **1987**, *1*, 95–114). It was speculated, on the basis of the intense UV absorptivity and the presence of aldehyde signals in the proton NMR spectrum, that rhizobactin 1021 may contain α,β-unsaturated functionalities. In the preparation of rhizobactin 1021 used for the structural elucidation presented here, an aldehyde peak of low intensity was observed by both ^1H (8.5 ppm) and ^{13}C (193.5 ppm) NMR. Based on NMR and mass spectroscopic evidence (not shown), it was, however, concluded that the aldehyde was present as part of a contaminant (≤5%).

(43) Linke, W.; Crueger, A.; Diekmann, H. *Arch. Mikrobiol.* **1972**, *85*, 44–50.

(44) Maurer, P. J.; Miller, M. J. *J. Am. Chem. Soc.* **1982**, *104*, 3096–3101.

(45) Ayorinde, F.; Wheeler, J. W.; Wemmer, C.; Murtaugh, J. *J. Chem. Ecol.* **1982**, *8*, 177–183.

(46) Boch, R.; Shearer, D. A.; Shuel, R. W. *J. Apic. Res.* **1979**, *18*, 250–253.

(47) Snow, G. A. *Bacteriol. Rev.* **1970**, *34*, 99–125. A minor component of the mycobactin F complex has been reported to contain a C-10 unsaturated fatty acid, configuration and position of the double bond unspecified.

(48) Anke, H.; Kinn, J.; Bergquist, K.-E.; Sterner, O. *Biol. Met.* **1991**, *4*, 176–180.

(49) de Lorenzo, V.; Bindereif, A.; Paw, B. H.; Neilands, J. B. *J. Bacteriol.* **1986**, *165*, 570–578.

(50) (a) Konopka, K.; Bindereif, A.; Neilands, J. B. *Biochemistry* **1982**, *24*, 6503–6508. (b) Warner, P. J.; Williams, P. J.; Bindereif, A.; Neilands, J. B. *Infect. Immun.* **1981**, *33*, 540–545.